

# Linear optical absorption spectra of mesoscopic structures in intense THz fields: free particle properties

Kristinn Johnsen<sup>1,2</sup> and Antti-Pekka Jauho<sup>1</sup>

<sup>1</sup>*Mikroelektronik Centret, Technical University of Denmark, Bldg 345east  
DK-2800 Lyngby, Denmark*

<sup>2</sup>*Dept. of Mathematics, University of California, Santa Barbara, CA93106, USA*

We theoretically study the effect of THz radiation on the linear optical absorption spectra of semiconductor structures. A general theoretical framework, based on non-equilibrium Green functions, is formulated, and applied to the calculation of linear optical absorption spectrum for several non-equilibrium mesoscopic structures. We show that a blue-shift occurs and sidebands appear in bulk-like structures, i.e., the dynamical Franz-Keldysh effect [A.-P. Jauho and K. Johnsen, Phys. Rev. Lett. **76**, 4576 (1996)]. An analytic calculation leads to the prediction that in the case of superlattices distinct stable steps appear in the absorption spectrum when conditions for dynamical localization are met.

PACS numbers: 71.10.-w, 78.20.Bh, 78.20.Jq, 78.47.+p

(Submitted to Physical Review B on April 3, 1997)

## I. INTRODUCTION

Light absorption can be described in terms of a process where polarization is induced in the medium. To linear order in the electric field component of the traversing light,  $\mathcal{E}$ , the induced polarizability,  $\mathcal{P}$ , can be expressed in terms of the dielectric susceptibility  $\chi$  as

$$\mathcal{P}(t) = \int_{-\infty}^t dt' \chi(t, t') \mathcal{E}(t').$$

If the absorbing medium is in a stationary state, the susceptibility depends only on the difference of its time arguments, i.e.,  $\chi(t, t') = \chi(t - t')$ . Under these conditions Maxwell's equation for  $\mathcal{E}$  is an algebraic equation in frequency space and one finds that the absorption is proportional to the imaginary part of  $\chi(\omega)$ . However, under non-equilibrium conditions, which are the topic of the present study, the susceptibility is a two-time function, and Maxwell's equation remains an integral equation even in the frequency domain. Further progress hinges upon two steps: first, one has to develop methods to calculate the non-equilibrium susceptibility function and second, one has to specify what sort of light wave or pulse is used in the absorption experiment. The present work addresses both of these problems. As far as the time-dependence of the probe pulse is concerned, two specific situations are examined. First, consider an undoped semiconductor placed in an intense THz field; we assume that the THz field is not able to induce polarization, i.e., no carriers are excited in the conduction band. Such a system is in a non-equilibrium state, i.e., the susceptibility is a two time function. Properties of such systems have been investigated experimentally using the Free Electron Laser (FEL) as a source for intense THz fields [1]; many interesting properties have been discovered, and others predicted, such as photon-assisted

tunneling [2], dynamical localization and absolute negative conductivity [3], ac Stark effect [4], dynamical Franz-Keldysh effect and formation of sidebands [5–8]. A second example consists of ultra-fast transients. Consider an undoped semiconductor structure subject to an external intense static field. At some time instant a population of carriers is pumped into the conduction band. These mobile charges will rearrange themselves so as to screen the external field. While the screening is building up the susceptibility of the system is a two time function. Using femtosecond laser techniques, which are able to probe the time scales in which screening is building up, experiments investigating the non-equilibrium properties of such systems have been performed [9,10].

Bandgap engineering techniques of semiconductor compounds, such as Molecular Beam Epitaxy (MBE), allow spatial modulation of the bandgap down to atomic resolution. It is possible to break the translational symmetries of bulk crystals, induce new ones and reduce the degrees of freedom with these techniques. Construction of systems which are effectively two dimensional (2D) and even one dimensional (1D) with regard to electron mobility and optical properties is today a standard procedure. Another example of such man-made structures are superlattices (SL), i.e., an engineered periodic potential in the growth direction of the sample. The interplay between the mesoscopic properties and the dynamical properties can lead to many interesting phenomena such as absolute negative resistance for the transport properties [11] and the rich features in the optical properties which are the subject of the present work.

The purpose of this paper is to present a theoretical study of light absorption in mesoscopic systems subject to intense THz [far infrared (FIR)] fields. We consider undoped systems, which implies that there are no carriers in the conduction band. Thus, the near infrared (NIR) inter-band absorption is the dominant absorption

process. The non-equilibrium nature of the system necessitates the use of special theoretical tools; we have chosen to apply the non-equilibrium Green function techniques [12,13]. In particular, this method allows us to treat the intense FIR field non-perturbatively, and defines a framework in which screening can be treated systematically. Our analysis consists of the following steps. Starting from a two-band Hamiltonian we derive a formal expression for the inter-band susceptibility in terms of non-equilibrium Green functions. Next, we use the general expression to derive the NIR absorption spectrum for non-interacting particles (Coulomb interactions will be discussed in a subsequent paper, see also below). Finally, we give explicit results for a number of special cases (3-, 2-, 1-d systems and superlattices), and discuss the physical implications.

This paper is organized as follows. In section II we derive a general expression for the two-time dielectric inter-band susceptibility. Section III relates the susceptibility to the measured absorption, considering both continuous wave measurements as well as short white light pulses. The single-particle Green functions and the corresponding spectral functions, which determine the susceptibility, are defined in section IV and related to the generalized density of states [6] (GDOS), which, in turn, is shown to determine the optical absorption. Section V considers bulk-like systems, and we obtain analytic results for the GDOS, which is analyzed in some detail in terms of the side-band picture. The properties of light absorption in superlattices are treated in section VI. Specific attention is paid to conditions where dynamical localization occurs, and we show how it affects the absorption spectrum. Finally, in section VII we have some concluding remarks.

## II. THE DIELECTRIC INTER-BAND SUSCEPTIBILITY

We shall now derive an expression for the dielectric inter-band susceptibility using non-equilibrium Green functions. The microscopic operator describing inter-band polarization is

$$\vec{P}(t) = \sum_k \vec{d}_k \left[ a_k^\dagger(t) b_k(t) + b_k^\dagger(t) a_k(t) \right]. \quad (1)$$

Here  $\vec{d}_k$  is the dipole matrix-element,  $a_k^\dagger(t)$  [ $a_k(t)$ ] are the conduction band electron creation [annihilation] operators and  $b_k^\dagger(t)$  [ $b_k(t)$ ] are the valence band creation [annihilation] operators. The linearized Hamiltonian associated with a polarization  $\vec{P}(t)$  induced by the external field  $\mathcal{E}(t)$  is  $H_P(t) = -\vec{P}(t) \cdot \mathcal{E}(t)$ . Linear response theory now yields the Cartesian  $l$ -component of the induced inter-band polarization due to a weak external field  $\mathcal{E}$ :

$$\mathcal{P}_l(t) = -\frac{i}{\hbar} \int_{-\infty}^{\infty} dt' \theta(t-t') \langle [\vec{P}(t'), P_l(t)] \rangle \cdot \mathcal{E}(t'). \quad (2)$$

The retarded susceptibility tensor can be identified from Eq.(2):

$$\chi_{lm}^r(t, t') = -\frac{i}{\hbar} \theta(t-t') \langle [P_m(t'), P_l(t)] \rangle. \quad (3)$$

Following the standard line of attack in non-equilibrium theory [12], we first consider the causal (time-ordered) response function:

$$\chi_{lm}^c(t, t') = -\frac{i}{\hbar} \langle T\{P_m(t') P_l(t)\} \rangle \quad (4)$$

where  $T$  is the time-ordering operator. In non-equilibrium, the causal response function is replaced by its contour ordered counterpart:  $\chi_{lm}^c(t, t') \rightarrow \chi_{lm}^c(\tau, \tau')$ , where the complex-time variables  $\tau, \tau'$  reside on the Keldysh contour. Finally we obtain the retarded tensor by an analytic continuation using the Langreth rules [14].

We use Eq.(1) to write the susceptibility as

$$\begin{aligned} \chi_{lm}^c(\tau, \tau') = & -\frac{i}{\hbar} \sum_{qk} d_l(k) d_m(q) \\ & \times [\langle T_c \{ a_q^\dagger(\tau') b_q(\tau') a_k^\dagger(\tau) b_k(\tau) \} \rangle \\ & + \langle T_c \{ a_q^\dagger(\tau') b_q(\tau') b_k^\dagger(\tau) a_k(\tau) \} \rangle \\ & + \langle T_c \{ b_q^\dagger(\tau') a_q(\tau') a_k^\dagger(\tau) b_k(\tau) \} \rangle \\ & + \langle T_c \{ b_q^\dagger(\tau') a_q(\tau') b_k^\dagger(\tau) a_k(\tau) \} \rangle]. \end{aligned} \quad (5)$$

where  $T_c$  is the contour-ordering operator. In equilibrium, the two-particle correlation functions occurring in Eq.(5) would be found via the Bethe-Salpeter equation [15]. In what follows, however, we shall consider the non-interacting limit of Eq.(5). This approach is motivated by the following considerations. The noninteracting limit will allow significant analytic progress, and the results, which we believe are interesting in their own right, will form the basis for any subsequent interacting theories. Secondly, experimentally it is known that in undoped semiconductor quantum wells excitons are quenched if the system is subject to intense FIR [16], thus implying that for the present situation Coulomb interactions may not play an equally dominant role as is the case in equilibrium situations. A quantitative assessment requires a non-equilibrium theory for the two-particle Green functions and will be a topic of our future work. For non-interacting particles we can use Wick's theorem to factorize the two-particle correlation functions. Thus, the non-equilibrium susceptibility can be expressed in terms of single-particle Green functions. The following Green functions are needed:

$$g_c(k, \tau; q, \tau') = -i \langle T_c \{ a_k(\tau) a_q^\dagger(\tau') \} \rangle \quad (6)$$

$$g_v(k, \tau; q, \tau') = -i \langle T_c \{ b_k(\tau) b_q^\dagger(\tau') \} \rangle \quad (7)$$

$$g_{ab}(k, \tau; q, \tau') = -i \langle T_c \{ a_k(\tau) b_q^\dagger(\tau') \} \rangle \quad (8)$$

and

$$g_{ba}(k, \tau; q, \tau') = -i\langle T_c \{b_k(\tau)a_q^\dagger(\tau')\} \rangle. \quad (9)$$

We assume that the frequency,  $\Omega$ , of the FIR field is such that  $\hbar\Omega \ll \epsilon_g$ . In typical experiments on III-V systems  $\epsilon_g$  is of the order of eV, while  $\hbar\Omega$  is a few meV, so this condition is satisfied. Consequently, inter-band transitions due to the perturbing field can be ignored, and the Green functions related to Zener-effect, i.e.,  $g_{ab}(k, \tau; q, \tau')$  and  $g_{ba}(k, \tau; q, \tau')$ , are neglected from this on. The first order non-equilibrium susceptibility reads thus

$$\begin{aligned} \chi_{lm}^c(\tau, \tau') = & -\frac{i}{\hbar} \sum_k d_l(k) d_m(q) [g_c(k, \tau; q, \tau') g_v(q, \tau'; k, \tau) \\ & + g_v(k, \tau; q, \tau') g_c(q, \tau'; k, \tau)]. \end{aligned} \quad (10)$$

The analytic continuation to real times is performed with the Langreth rules [14], which state that if on contour

$$C(\tau, \tau') = A(\tau, \tau') B(\tau', \tau), \quad (11)$$

then the retarded function on the real time axis is

$$C^r(t, t') = A^<(t, t') B^a(t', t) + A^r(t, t') B^<(t', t). \quad (12)$$

We thus have

$$\begin{aligned} \chi_{lm}^r(t, t') = & -\frac{i}{\hbar} \sum_k d_l(k) d_m(k) [g_c^<(k, t, t') g_v^a(k, t', t) \\ & + g_c^r(k, t, t') g_v^<(k, t', t) + g_v^<(k, t, t') g_c^a(k, t', t) \\ & + g_v^r(k, t, t') g_c^<(k, t', t)], \end{aligned} \quad (13)$$

with

$$g^<(t, t') = i\langle c^\dagger(t') c(t) \rangle, \quad (14)$$

$$g^a(t, t') = i\theta(t' - t)\langle\{c(t), c^\dagger(t')\}\rangle, \quad (15)$$

$$g^r(t, t') = -i\theta(t - t')\langle\{c(t), c^\dagger(t')\}\rangle. \quad (16)$$

We recall the following relations:

$$\begin{aligned} [g^<(t, t')]^* &= -g^<(t', t) \\ [g^a(t, t')]^* &= g^r(t', t) \\ [g^r(t, t')]^* &= g^a(t', t) \end{aligned} \quad (17)$$

For certain applications, e.g. Section III A, it is convenient to introduce the center of mass variables  $T = (t' + t)/2$  and  $\tau = t - t'$  [17]. In terms of these variables the symmetry relations of the Green functions are:

$$\begin{aligned} [g^<(T, \tau)]^* &= -g^<(T, -\tau) \\ [g^a(T, \tau)]^* &= g^r(T, -\tau) \\ [g^r(T, \tau)]^* &= g^a(T, -\tau) \end{aligned} \quad (18)$$

The retarded susceptibility expressed in center of mass coordinates is

$$\begin{aligned} \chi_{lm}^r(T, \tau) = & -\frac{i}{\hbar} \sum_k d_l(k) d_m(k) \\ & \times \{[g_c^<(k, T, \tau) g_v^a(k, T, -\tau) \\ & + g_v^<(k, T, \tau) g_c^a(k, T, -\tau)] - h.c.\}. \end{aligned} \quad (19)$$

Note that in equilibrium  $\chi_{lm}^r(T, \tau) = \chi_{lm}^r(\tau)$ . As shown in Section III A, the relevant quantity for continuous wave measurements at frequency  $\omega_l$  is

$$\text{Im}\chi_{lm}^r(T, \omega_l) = \text{Im} \left\{ \int_{-\infty}^{\infty} d\tau e^{i\omega_l \tau} \chi_{lm}^r(T, \tau) \right\} \quad (20)$$

to first order in  $\Omega/\omega_l$  (here  $\Omega$  is the FIR frequency). Now,  $\chi_{lm}^r(T, \tau)$  is a real quantity as is evident from (19). Using the properties of the Fourier transform we obtain

$$\begin{aligned} \chi_{lm}^r(T, \omega_l) = & -\frac{i}{\hbar} \sum_k d_l(k) d_m(k) \int_{-\infty}^{\infty} \frac{d\omega}{2\pi} \{ g_c^<(k, T, \omega) \\ & \times [g_v^a(k, T, \omega - \omega_l) + g_v^r(k, T, \omega + \omega_l)] \\ & + g_v^<(k, T, \omega) \\ & \times [g_c^a(k, T, \omega - \omega_l) + g_c^r(k, T, \omega + \omega_l)] \}. \end{aligned} \quad (21)$$

Since  $\chi_{lm}^r(T, \tau)$  is real, the imaginary part of its Fourier transform is obtained through

$$\text{Im}\chi_{lm}^r(T, \omega_l) = \frac{1}{2i} [\chi_{lm}^r(T, \omega_l) - \chi_{lm}^r(T, -\omega_l)]. \quad (22)$$

We can therefore write, in terms of the spectral functions

$$A_c(k, T, \omega) = i[g_c^r(k, T, \omega) - g_c^a(k, T, \omega)] \quad (23)$$

and

$$A_v(k, T, \omega) = i[g_v^r(k, T, \omega) - g_v^a(k, T, \omega)], \quad (24)$$

that

$$\begin{aligned} \text{Im}\chi_{lm}^r(T, \omega_l) = & \frac{i}{2\hbar} \sum_k d_l(k) d_m(k) \int_{-\infty}^{\infty} \frac{d\omega}{2\pi} \{ g_c^<(k, T, \omega) \\ & \times [A_v(k, T, \omega - \omega_l) - A_v(k, T, \omega + \omega_l)] \\ & + g_v^<(k, T, \omega) \\ & \times [A_c(k, T, \omega - \omega_l) - A_c(k, T, \omega + \omega_l)] \}. \end{aligned} \quad (25)$$

The lesser functions can be expressed in the form [12]

$$g_a^<(k, T, \omega) = i f_a(k, T, \omega) A_a(k, T, \omega) \quad (26)$$

where  $f_a(k, T, \omega)$  is a generalized particle distribution for particles of species  $a$ , and  $A_a(k, T, \omega)$  is the corresponding spectral function. In accordance with our assumption about no FIR field induced inter-band transitions, we can set  $f_c(k, T, \omega) = 0$  (zero occupation of conduction band), and that  $f_v(k, T, \omega) = 1$  (all valence states are occupied). In the general case, e.g., when considering nonlinear effects in the *probing* light field, one would have to find  $f_a(k, T, \omega)$  via, say, a Monte Carlo solution of semiconductor Bloch equations [18,19] or by a direct integration of quantum kinetic equations for  $g_a^<(k, T, \omega)$  [12]. With these assumptions the susceptibility reduces to

$$\begin{aligned}
\text{Im}\chi_{lm}^r(T, \omega_l) &= \frac{-1}{2\hbar} \sum_k d_l(k) d_m(k) \int_{-\infty}^{\infty} \frac{d\omega}{2\pi} A_v(k, T, \omega) \\
&\quad \times \{A_c(k, T, \omega - \omega_l) - A_c(k, T, \omega + \omega_l)\} \\
&= \frac{1}{2\hbar} \sum_k d_l(k) d_m(k) \\
&\quad \times \int_{-\infty}^{\infty} \frac{d\omega}{2\pi} A_v(k, T, \omega) A_c(k, T, \omega + \omega_l).
\end{aligned} \tag{27}$$

The second equality comes about because we do not consider overlapping bands. Eq.(27), which is the central result of this section, expresses the fact that the non-equilibrium inter-band susceptibility function can be calculated from a *joint spectral function*, which is a convolution of the individual band spectral function. A similar result is known from high-field quantum transport theory [20]: there the field-dependent scattering rate is expressed as a joint spectral function for the initial and final states.

In order to make a connection to the equilibrium case, we recall the exact identity  $g_{\text{eq}}^<(k, \omega) = ia_{\text{eq}}(k, \omega)n(\omega)$  ( $n(\omega)$  is the Fermi function), and obtain from Eq.(25) [15,21]

$$\begin{aligned}
\text{Im}\chi_{lm}^r(\omega_l) &= -\frac{1}{2\hbar} \sum_k d_l(k) d_m(k) \\
&\quad \times \int_{-\infty}^{\infty} \frac{d\omega}{2\pi} \left\{ n_c(\omega) a_{c,\text{eq}}(k, \omega) \right. \\
&\quad \times [a_{v,\text{eq}}(k, \omega - \omega_l) - a_{v,\text{eq}}(k, \omega + \omega_l)] \\
&\quad + n_v(\omega) a_{v,\text{eq}}(k, \omega) \\
&\quad \left. \times [a_{c,\text{eq}}(k, \omega - \omega_l) - a_{c,\text{eq}}(k, \omega + \omega_l)] \right\}.
\end{aligned} \tag{28}$$

Here  $n_c(\omega)$  is the conduction band electron occupation function, and  $n_v(\omega)$  is corresponding function for the valence band electrons.

### III. ABSORPTION COEFFICIENT IN TERMS OF THE TIME DEPENDENT DIELECTRIC SUSCEPTIBILITY

The dielectric susceptibility  $\chi$  links the induced polarization  $\mathcal{P}$  to the field  $\mathcal{E}$  via

$$\mathcal{P}(t) = \int_{-\infty}^t dt' \chi(t, t') \mathcal{E}(t'). \tag{29}$$

The wave equation for light is then

$$\nabla^2 \mathcal{E}(t) - \frac{1}{c^2} \frac{\partial^2 \mathcal{D}(t)}{\partial t^2} = 0 \tag{30}$$

where  $\mathcal{D}(t) = \mathcal{E}(t) + 4\pi\mathcal{P}(t)$ . The absorption coefficient  $\alpha(\omega)$  is defined as the inverse of the length which light

has to traverse in the medium at frequency  $\omega$  in order for the intensity of the light to decrease by a factor of  $1/e$ . In equilibrium  $\mathcal{D}(\omega) = [1 + 4\pi\chi(\omega)]\mathcal{E}(\omega) = \epsilon(\omega)\mathcal{E}(\omega)$  and the absorption coefficient [18] becomes

$$\alpha(\omega) = 4\pi\omega \frac{\text{Im}\chi(\omega)}{cn(\omega)}. \tag{31}$$

Here  $n^2(\omega) = \frac{1}{2}[\text{Re}\epsilon(\omega) + |\epsilon(\omega)|]$  is the refraction coefficient which usually depends only weakly on  $\omega$ . In non-equilibrium this analysis must be generalized, and we consider two special cases: (i) monochromatic continuous wave measurements, and (ii) white light short pulse measurements.

#### A. Continuous wave measurements

Consider a system out of equilibrium which is probed by a light field (which is assumed to be weak) of frequency  $\omega_l$ :

$$\mathcal{E}(r, t) = \mathcal{E}_0 \exp[i(r \cdot k - \omega_l t)]. \tag{32}$$

The polarization can then be expressed as

$$\mathcal{P}(t) = \mathcal{E}(r, t) \int_{-\infty}^{\infty} dt' e^{i\omega_l(t-t')} \chi^r(t, t'). \tag{33}$$

This form is suggestive: it is advantageous to express  $\chi^r$  in terms of the center-of-mass and difference coordinates,  $\chi^r(t, t') \rightarrow \tilde{\chi}^r(\frac{1}{2}(t+t'), t-t')$ . The characteristic time-scale for the center-of-mass time is set by the “slow” frequency  $\Omega$ , while the difference-time varies on the scale of the “fast” frequency  $\omega_l$ . We thus gradient-expand:  $\tilde{\chi}^r(\frac{1}{2}(t+t'), t-t') \simeq \tilde{\chi}^r(t, t-t') + \frac{1}{2}(t'-t)\tilde{\chi}^{r'}(t, t-t') + \dots$ , where the prime indicates differentiation with respect to the slow temporal variable. Substitution in (33) then yields (we introduce a new variable  $\tau \equiv t - t'$ )

$$\begin{aligned}
\mathcal{P}(t) &= \mathcal{E}(r, t) \int d\tau e^{i\omega_l\tau} [\tilde{\chi}^r(t, \tau) + (-\frac{1}{2}\tau)\tilde{\chi}^{r'}(t, \tau) + \dots] \\
&= \mathcal{E}(r, t) [\tilde{\chi}^r(t, \omega_l) + \frac{\partial}{\partial\omega_l} \frac{\partial}{\partial t} \frac{i}{2} \tilde{\chi}^r(t, \omega_l) + \dots] \\
&= \mathcal{E}(r, t) \exp \left[ \frac{i}{2} \frac{\partial^2}{\partial t \partial \omega_l} \right] \tilde{\chi}^r(t, \omega_l).
\end{aligned} \tag{34}$$

Eq.(34) can now be used in the Maxwell equation; note however that upon Fourier-transforming the dominant frequency comes from  $\mathcal{E}(t)$  and we can keep  $t$  in  $\chi(t, \omega_l)$  fixed. The slow time-variation will from this on be indicated by  $T$ . Proceeding as in deriving the static result (31), we identify the *time-dependent* absorption coefficient

$$\alpha_T(\omega) = 4\pi\omega \frac{\text{Im}\tilde{\chi}^r(T, \omega)}{cn_T(\omega)} + \mathcal{O}(\Omega/\omega). \tag{35}$$

If the driving force is periodic in  $T$  (the harmonic time-dependence due to a FEL-laser is an important special case), then the average absorption coefficient is

$$\begin{aligned}\bar{\alpha}(\omega) &= \frac{1}{T_{\text{period}}} \int_{\text{period}} dT \alpha_T(\omega) \\ &= \frac{1}{T_{\text{period}}} \int_{\text{period}} dT 4\pi\omega \frac{\text{Im}\tilde{\chi}^r(T, \omega)}{cn_T(\omega)}\end{aligned}\quad (36)$$

to *all* orders in  $\Omega/\omega$ . We stress that here  $\tilde{\chi}^r(T, \omega)$  is Fourier transformed with respect to the difference variable  $\tau$ . Below we shall represent numerical examples for the generalized absorption coefficient.

### B. Short white light pulse measurements

Consider now an instantaneous measurement performed on a non-equilibrium system: at some specific time  $t = t_m$  the system is probed with a weak pulse whose duration is short compared to the characteristic dynamics of the system. We approximate the pulse with delta function in time:

$$\mathcal{E}(r, t) = \mathcal{E}_0 e^{ir \cdot k} \delta(t - t_m). \quad (37)$$

In principle, construction of such a pulse would take infinite energy due to its time dependence. The pulse is therefore hardly “weak”. When we refer to the pulse as weak we assume that  $\mathcal{E}_0 \ll 1$ , that is the intensity of the light is small at all frequencies. Using (37) in the Maxwell equation yields dispersion relation

$$k^2 = \frac{\omega^2}{c^2} [1 + 4\pi\chi^r(\omega, t_m)]. \quad (38)$$

This dispersion relation looks quite similar to the one obtained in the previous section. The difference is that here  $\chi^r(\omega, t_m)$  is Fourier transformed with respect to  $t'$ , *not* the difference variable  $\tau$ . In the present case we obtain the time dependent absorption coefficient

$$\alpha_t(\omega) = 4\pi\omega \frac{\text{Im}\chi^r(\omega, t)}{cn_t(\omega)}. \quad (39)$$

For examples of experiments which probe systems in this manner see, e.g., Refs. [9,10].

### C. Differential Transmission Spectrum

Consider a sample of thickness  $L$ ; then the ratio of the intensity transmitted through the sample with its initial intensity is  $T(\omega) = \exp[-\bar{\alpha}(\omega)L]$  where  $\bar{\alpha}(\omega)$  is the absorption coefficient of the sample. Experimental setups for measuring the change in absorption due to externally controlled perturbations commonly measure the differential transmission spectrum (DTS) defined by [18]

$$DTS(\omega) = \frac{T(\omega) - T_0(\omega)}{T_0(\omega)}. \quad (40)$$

Here  $T(\omega)$  is the transmission with the perturbation present and  $T_0(\omega)$  is the transmission through the unperturbed sample. Below we give examples of  $DTS(\omega)$  in non-equilibrium situations.

## IV. SINGLE PARTICLE GREEN FUNCTIONS AND THE SPECTRAL FUNCTIONS

In this section we determine the single-particle Green functions and their associated spectral functions. We show that, under conditions specified below, that the convolutions of the spectral functions, encountered in Section II, result in effective single band spectral functions.

### A. The single particle Green functions

Let  $\vec{A}$  be the vector potential which defines the FIR field. Considering harmonic, translationally invariant external fields we choose

$$\vec{A}(t) = -\vec{E} \frac{\sin(\Omega t)}{\Omega}, \quad (41)$$

which represents the physical uniform electric field  $\vec{E} \cos(\Omega t)$ . The Hamiltonian describing the two bands is then

$$H = \sum_{\vec{k}} \left\{ \epsilon_c [\vec{k} - e\vec{A}(t)] a_{\vec{k}}^\dagger a_{\vec{k}} + \epsilon_v [\vec{k} - e\vec{A}(t)] b_{\vec{k}}^\dagger b_{\vec{k}} \right\}. \quad (42)$$

The Dyson equation for the retarded/advanced free-particle Green function is

$$\left( i\hbar \frac{\partial}{\partial t} - \epsilon_{\alpha} [\vec{k} - e\vec{A}(t)] \right) g_{\alpha}^{r/a}(\vec{k}, t, t') = \delta(t - t'), \quad (43)$$

where  $\alpha \in \{c, v\}$  is the band index. This equation is readily integrated with the solutions

$$g_{\alpha}^{r/a}(\vec{k}, t, t') = \mp \frac{i}{\hbar} \theta(\pm t \mp t') \exp \left\{ -\frac{i}{\hbar} \int_{t'}^t ds \epsilon_{\alpha} [\vec{k} - e\vec{A}(s)] \right\}, \quad (44)$$

and the spectral function  $A = i(g^r - g^a)$  becomes

$$A_{\alpha}(\vec{k}, t, t') = \frac{1}{\hbar} \exp \left\{ -\frac{i}{\hbar} \int_{t'}^t ds \epsilon_{\alpha} [\vec{k} - e\vec{A}(s)] \right\}. \quad (45)$$

## B. Convolution of the spectral functions

According to Section II the susceptibility is obtained through the trace of a convolution of the spectral functions. We shall now show that within the present model the convolution of spectral functions results in a new effective single-band spectral function.

In terms of the center of mass variables,  $\tau = t - t'$  and  $T = (t + t')/2$ , we write the spectral functions as

$$A_\alpha(\vec{k}, T, \omega) = \frac{1}{\hbar} \int_{-\infty}^{\infty} d\tau e^{i\omega\tau} \times \exp \left\{ -\frac{i}{\hbar} \int_{T-\tau/2}^{T+\tau/2} ds \epsilon_\alpha[\vec{k} - e\vec{A}(s)] \right\}. \quad (46)$$

Then the convolution,

$$b(\vec{k}, T, \omega_l) = \hbar \int_{-\infty}^{\infty} \frac{d\omega}{2\pi} A_e(\vec{k}, T, \omega) A_v(\vec{k}, T, \omega - \omega_l), \quad (47)$$

of the two spectral functions becomes

$$b(\vec{k}, T, \omega_l) = \frac{1}{\hbar} \int_{-\infty}^{\infty} d\tau e^{i\omega_l\tau} \exp \left\{ -\frac{i}{\hbar} \int_{T-\tau/2}^{T+\tau/2} ds (\epsilon_c[\vec{k} - e\vec{A}(s)] - \epsilon_v[\vec{k} - e\vec{A}(s)]) \right\}. \quad (48)$$

In the case of parabolic bands we have

$$\epsilon_c[\vec{k}] = \frac{\hbar^2 k^2}{2m_e} \quad , \quad \epsilon_v[\vec{k}] = -\frac{\hbar^2 k^2}{2m_h} - \epsilon_g. \quad (49)$$

Here  $m_e$  is the electron mass,  $m_h$  is the positive hole mass and  $\epsilon_g$  is the band gap. We define a single effective band for the system:

$$\epsilon_{\text{eff}}[\vec{k}] \equiv \epsilon_c[\vec{k}] - \epsilon_v[\vec{k}] = \frac{\hbar^2 k^2}{2m_{\text{eff}}} + \epsilon_g, \quad (50)$$

where  $m_{\text{eff}} = m_e m_h / (m_e + m_h)$  is the effective reduced mass. Thus, the effective band is parabolic like the original bands but with their reduced mass. It is therefore evident that the convolution, writing  $A_{\text{eff}}(\vec{k}, T, \omega_l) = b(\vec{k}, T, \omega_l)$ , is a spectral function for a parabolic band,

$$A_{\text{eff}}(\vec{k}, T, \omega) = \frac{1}{\hbar} \int_{-\infty}^{\infty} d\tau e^{i\omega\tau} \times \exp \left\{ -\frac{i}{\hbar} \int_{T-\tau/2}^{T+\tau/2} ds \epsilon_{\text{eff}}[\vec{k} - e\vec{A}(s)] \right\}. \quad (51)$$

In the case of tight-binding minibands for a type I superlattice (with period  $a$ ) we write the bands as

$$\epsilon_c[\vec{k}] = \frac{1}{2} \lambda_c \cos(ak_{\parallel}) + \frac{\hbar^2 k_{\perp}^2}{2m_e} \quad (52)$$

$$\epsilon_v[\vec{k}] = -\frac{1}{2} \lambda_v \cos(ak_{\parallel}) - \frac{\hbar^2 k_{\perp}^2}{2m_h} - \epsilon_g, \quad (53)$$

where  $\lambda_c$  is the electron miniband width,  $\lambda_h$  is the corresponding bandwidth for the holes;  $k_{\parallel}$  is the (crystal) momentum component parallel to the growth direction of the superlattice and  $k_{\perp}$  is the magnitude of the component perpendicular to the growth direction. The effective band thus becomes

$$\epsilon_{\text{eff}}[\vec{k}] = \frac{1}{2} \lambda_{\text{eff}} \cos(ak_{\parallel}) + \frac{\hbar^2 k_{\perp}^2}{2m_{\text{eff}}} + \epsilon_g, \quad (54)$$

where  $\lambda_{\text{eff}} = \lambda_c + \lambda_v$  is the effective bandwidth, which again is of the same form as the original bands. This shows that also for superlattices the convolution (47) leads to an effective spectral function of the original form.

In terms of the effective spectral function the imaginary part of the susceptibility can be written as

$$\text{Im}\chi_{lm}^r(T, \omega_l) = \frac{d_l d_m}{2\hbar} \sum_{\vec{k}} A_{\text{eff}}(\vec{k}, T, \omega_l), \quad (55)$$

where we assume that the dipole matrix elements are  $k$ -independent. In equilibrium the trace of the spectral function yields the density of states for the system. Analogously, the *generalized time-dependent density of states* (GDOS) [6] is defined as

$$\rho(T, \omega_l) = \frac{1}{\pi} \sum_{\vec{k}} A_{\text{eff}}(\vec{k}, T, \omega_l), \quad (56)$$

allowing us to write the absorption coefficient as

$$\alpha_T(\omega_l) \approx \frac{2\pi^2 \omega_l |d|^2}{cn\hbar} \rho(T, \omega_l). \quad (57)$$

For the remainder of this work we shall investigate the properties of  $\rho(T, \omega_l)$  for various systems.

## C. Gauge invariance

To conclude this section we briefly comment on gauge invariance. We might have, from the outset, chosen to work within the gauge invariant formulation which has been developed in of high-field transport [22,23,12]. Considering translationally invariant systems, correlation functions are made gauge invariant with the transformation

$$\vec{k} \rightarrow \vec{k} + \frac{e}{t - t'} \int_{t'}^t ds \vec{A}(s). \quad (58)$$

However, the absorption coefficient follows from a trace operation (56), which makes the transformation (58) redundant: a simple change of variables when performing the trace undoes (58) and proves that our formulation of the absorption is gauge invariant.

## V. PARABOLIC BANDS

In this section we shall investigate the properties of the generalized density of states for systems which can be effectively described by Hamiltonians yielding parabolic bands, be it in one, two or three dimensions. We write the effective single-band dispersion as

$$\epsilon[\vec{k}] = \frac{\hbar^2 k^2}{2m_{\text{eff}}} + \epsilon_g. \quad (59)$$

For convenience we write  $m = m_{\text{eff}}$  and set  $\epsilon_g = 0$  which shifts the energy axis such that the reference point is the band gap energy. We calculate the generalized density of states from

$$\rho^{nD}(T, \epsilon) = \int_{-\infty}^{\infty} d\tau e^{i\epsilon\tau/\hbar} \rho^{nD}(T, \tau), \quad (60)$$

where

$$\rho^{nD}(T, \tau) = \frac{1}{\hbar} \int \frac{d^n \vec{k}}{(2\pi)^n} \exp \left\{ -\frac{i}{\hbar} \int_{T-\tau/2}^{T+\tau/2} ds \epsilon[\vec{k} - e\vec{A}(s)] \right\}. \quad (61)$$

With the vector potential (41) one obtains explicitly that

$$\begin{aligned} \rho^{nD}(T, \tau) = & \frac{1}{\hbar} \int \frac{d^n \vec{k}}{(2\pi)^n} \exp \left\{ -i[(\epsilon_k + \epsilon_f)\tau/\hbar \right. \\ & + 2 \frac{e\vec{k} \cdot \vec{E}}{m\Omega^2} \sin(\Omega T) \sin\left(\frac{\Omega\tau}{2}\right) \\ & \left. - \frac{\omega_f}{\Omega} \cos(2\Omega T) \sin(\Omega\tau) \right\}. \end{aligned} \quad (62)$$

Here  $\epsilon_k = \hbar^2 k^2 / 2m$  and we have defined the fundamental energy scale

$$\epsilon_f = \hbar\omega_f = \frac{e^2 E^2}{4m\Omega^2}. \quad (63)$$

The energy  $\epsilon_f$  can be interpreted classically in the following way: consider a classical particle with charge  $e$  and mass  $m$  subjected to an electric field  $\vec{E}(t) = \vec{E} \cos(\Omega t)$ . From Newton's equation of motion one finds that the mean kinetic energy of such a particle equals  $\epsilon_f$ .

In order to perform the Fourier-transform (60) we utilize the identity [24]

$$\exp(ix \sin \theta) = \sum_n J_n(x) \exp(in\theta), \quad (64)$$

where  $J_n(x)$  are Bessel functions; we shall henceforth write  $\sum_n \equiv \sum_{n=-\infty}^{\infty}$  to simplify the notation. The generalized density of states becomes

$$\begin{aligned} \rho^{nD}(T, \epsilon) = & \sum_{l,j} \int \frac{d^n \vec{k}}{(2\pi)^{n-1}} \delta[\epsilon - \epsilon_k - \epsilon_f + l\hbar\Omega] \\ & \times J_{2j} \left( 2 \frac{e\vec{k} \cdot \vec{E}}{m\Omega^2} \sin(\Omega T) \right) \\ & \times J_{l+j} \left( \frac{\omega_f}{\Omega} \cos(2\Omega T) \right), \end{aligned} \quad (65)$$

The dimensionality is entirely contained in the remaining momentum integration  $\int d^n \vec{k} / (2\pi)^{n-1}$ . We note that Eq.(65) implies a shift of the absorption edge by  $\epsilon_f$ . The term  $l\hbar\Omega$  in the Dirac-delta function gives rise to photonic side bands. Since  $J_{2l}(x)$  is an even function, the density of states is invariant under the transformation  $\vec{E} \rightarrow -\vec{E}$ , as expected. In the following subsections we shall consider the 1D, 2D and 3D systems separately and show how the density of states smoothly evolves from a low field intensity regime into a high field intensity regime making the non-linear effects of the THz field apparent.

### A. Generalized density of states, 1D

The density of states for a single-mode 1D-system (“quantum wire”) in the absence of external fields is

$$\rho_0^{1D}(T, \epsilon) = \frac{1}{\pi} \left( \frac{2m}{\hbar^2} \right)^{1/2} \epsilon^{-1/2} \theta(\epsilon). \quad (66)$$

In the presence of a external strong oscillating field we get from (65) that the GDOS is

$$\begin{aligned} \rho^{1D}(T, \epsilon) = & \sum_{l,j} \int_{-\infty}^{\infty} dk \delta[\epsilon - \epsilon_k - \epsilon_f + l\hbar\Omega] \\ & \times J_{2j} \left( \frac{\sqrt{32\epsilon_f \epsilon_k}}{\hbar\Omega} \sin(\Omega T) \right) \\ & \times J_{l+j} \left( \frac{\epsilon_f}{\hbar\Omega} \cos(2\Omega T) \right) \\ = & \sum_l r_l^{1D}(T, \epsilon - \epsilon_f + l\hbar\Omega) \rho_0^{1D}(\epsilon - \epsilon_f + l\hbar\Omega), \end{aligned} \quad (67)$$

where the side-band weights are

$$\begin{aligned} r_l^{1D}(T, \epsilon) = & \sum_j J_{2j} \left( \frac{\sqrt{32\epsilon_f \epsilon}}{\hbar\Omega} \sin(\Omega T) \right) \\ & \times J_{l+j} \left( \frac{\epsilon_f}{\hbar\Omega} \cos(2\Omega T) \right). \end{aligned} \quad (68)$$

We note that in the limit  $\epsilon_f \rightarrow 0$

$$r_l^{1D}(T, \epsilon) \rightarrow \delta_{l,0} \quad (69)$$

and  $\rho^{1D}(T, \epsilon) \rightarrow \rho_0^{1D}(\epsilon)$ , as expected. If  $\Omega$  is in the THz regime then most experiments would probe the time averaged absorption. The time-average of the side-band weights is calculated from

$$\begin{aligned} \bar{r}_l^{1D}(\epsilon) = & \sum_j \int_0^{2\pi} \frac{ds}{2\pi} J_{2j} \left( \frac{\sqrt{32\epsilon_f \epsilon}}{\hbar\Omega} \sin(s) \right) \\ & \times J_{l+j} \left( \frac{\epsilon_f}{\hbar\Omega} \cos(2s) \right), \end{aligned} \quad (70)$$

which yields for  $l$  odd:

$$\bar{r}_l^{1D}(\epsilon) = \sum_j \int_0^{2\pi} \frac{ds}{2\pi} J_{4j+2} \left( \frac{\sqrt{32\epsilon_f\epsilon}}{\hbar\Omega} \sin(s) \right) \times J_{2j+l+1} \left( \frac{\epsilon_f}{\hbar\Omega} \cos(2s) \right), \quad (71)$$

and for  $l$  even

$$\bar{r}_l^{1D}(\epsilon) = \sum_j \int_0^{2\pi} \frac{ds}{2\pi} J_{4j} \left( \frac{\sqrt{32\epsilon_f\epsilon}}{\hbar\Omega} \sin(s) \right) \times J_{2j+l} \left( \frac{\epsilon_f}{\hbar\Omega} \cos(2s) \right). \quad (72)$$

At the onset of side band  $l$  the side-band weight is

$$\bar{r}_l^{1D}(0) = \begin{cases} 0 & \text{if } l \text{ odd} \\ J_{l/2}^2(\epsilon_f/\hbar\Omega) & \text{if } l \text{ even,} \end{cases} \quad (73)$$

where we used the identity [24]

$$\int_0^{2\pi} d\theta J_{2l}(a \cos \theta) = 2\pi J_l^2(a). \quad (74)$$

This shows that processes involving an odd number of photons of the THz field are strongly suppressed. In Fig. 1 we illustrate  $\rho_{\text{ave}}^{1D}(\epsilon)$  for a range of values of  $\epsilon_f/\hbar\Omega$ . In the figures we write  $\epsilon_e = \hbar\Omega$ . We observe all the signatures of the Dynamical Franz-Keldysh effect (DFK) [6]: Stark-like blue shift of the main absorption-edge by  $\epsilon_f$ , formation of side-bands at  $\epsilon_g + \epsilon_f \pm N\hbar\Omega$ , and finite absorption within the band-gap.

## B. Generalized density of states, 2D

Several authors have considered fields perpendicular to the quantum well, cf. [25] and references in these papers; here we focus on the situation where the electric field is in the plane of the two-dimensional electron gas. In such a system with no external field the density of states is constant,

$$\rho_0^{2D}(\epsilon) = \frac{m}{\pi\hbar^2} \theta(\epsilon). \quad (75)$$

With a harmonically oscillating field we obtain from (65)

$$\rho^{2D}(T, \epsilon) = \sum_{l,j} \int_0^\infty dk k \int_0^{2\pi} \frac{d\theta}{2\pi} \delta[\epsilon - \epsilon_k - \epsilon_f + l\hbar\Omega] \times J_{2j} \left( \frac{\sqrt{32\epsilon_f\epsilon_k}}{\hbar\Omega} \cos \theta \sin(\Omega T) \right) \times J_{l+j} \left( \frac{\epsilon_f}{\hbar\Omega} \cos(2\Omega T) \right). \quad (76)$$

The integrals in (76) are again performed using (74) and writing the result in the side-band picture we obtain [26]

$$\rho^{2D}(T, \epsilon) = \sum_l r_l^{2D}(T, \epsilon - \epsilon_f + l\hbar\Omega) \rho_0^{2D}(\epsilon - \epsilon_f + l\hbar\Omega) \quad (77)$$

where the side-band weights are

$$r_l^{2D}(T, \epsilon) = \sum_j J_j^2 \left( \frac{\sqrt{32\epsilon_f\epsilon}}{\hbar\Omega} \sin(\Omega T) \right) \times J_{l+j} \left( \frac{\epsilon_f}{\hbar\Omega} \cos(2\Omega T) \right). \quad (78)$$

Identical arguments as in the 1D case lead to

$$\bar{r}_l^{2D}(0) = \begin{cases} 0 & \text{if } l \text{ odd} \\ J_{l/2}^2(\epsilon_f/\hbar\Omega) & \text{if } l \text{ even,} \end{cases} \quad (79)$$

i.e., the same result as in the 1D-case.

As in the 1D case we have numerically investigated the time averaged GDOS  $\rho_{\text{ave}}^{2D}(\epsilon) = \frac{\Omega}{2\pi} \int_0^{2\pi/\Omega} dT \rho^{2D}(T, \epsilon)$ . In Fig. 2 we illustrate  $\rho_{\text{ave}}^{2D}(\epsilon)$  for various values of  $\epsilon_f/\hbar\Omega$ . Again, as in the 1D case, we observe all the characteristics of the DFK [6]. Finally, Fig. 3 shows the differential transmission (DTS) signal.

## C. Generalized density of states, 3D

Absorption in bulk semiconductors subject to THz radiation was considered already long time ago by Yacoby [5]. He studied transition rates between bands by investigating approximate solutions to the corresponding time-dependent Schrödinger equation. He concluded that transitions occur in the gap and noted reduced rates above the gap, both in agreement with the present work. General quantitative results, were not presented. The 3D field-free density of states is

$$\rho_0^{3D}(\epsilon) = \frac{1}{2\pi^2} \left( \frac{2m}{\hbar} \right)^{3/2} \theta(\epsilon) \epsilon^{1/2}. \quad (80)$$

With the external field the density of states becomes

$$\rho^{3D}(T, \epsilon) = \sum_l r_l^{3D}(T, \epsilon - \epsilon_f + l\hbar\Omega) \rho_0^{3D}(\epsilon - \epsilon_f + l\hbar\Omega), \quad (81)$$

with the side-band weights

$$r_l^{3D}(T, \epsilon) = \sum_j J_{l+j} \left( \frac{\epsilon_f}{\hbar\Omega} \cos(2\Omega T) \right) \times \int_0^1 d\eta J_{2j} \left( \frac{\sqrt{32\epsilon_f\epsilon}}{\hbar\Omega} \sin(\Omega T) \eta \right). \quad (82)$$

Again, we have

$$\bar{r}_l^{3D}(0) = \begin{cases} 0 & \text{if } l \text{ odd} \\ J_{l/2}^2(\epsilon_f/\hbar\Omega) & \text{if } l \text{ even.} \end{cases} \quad (83)$$

In Fig. 4 we illustrate  $\rho_{\text{ave}}^{3D}(\epsilon)$  for various values of  $\epsilon_f/\hbar\Omega$ ; the DTS signal for the 3D case is shown in Fig. 5.

## D. Summary

The main physical consequences of the THz field on linear absorption spectrum for systems with parabolic dispersion can be summarized as follows. The dynamical modifications of the absorption spectrum (i) Appear near the absorption edge; (ii) They extend a few  $\epsilon_e = \hbar\Omega$  around the edge, and (iii) They are most pronounced when  $\omega_f/\Omega$  is of order unity.

If  $\Omega$  is in the THz regime, and fields like those attainable with free electron lasers are considered [2,27], then  $\omega_f/\Omega \approx 1$  and the fine structure extends over an area of several meV. Consequently, an experimental verification of these effects should be possible.

## VI. SUPERLATTICES

According to the semiclassical Bloch-Boltzmann theory of transport, a uniform electric field causes charge carriers in a periodic potential to execute a time-periodic motion with frequency  $\omega_B = eaE/\hbar$ , where  $a$  is the lattice periodicity. Conditions for observing these Bloch oscillations are much more favorable in superlattices than in ordinary bulk materials, and recent years have witnessed an intense research effort culminating in the observation of Bloch oscillations [28]. In ac-fields a phenomenon called dynamical localization may occur: if the parameter  $\gamma \equiv aeE_{\parallel}/\hbar\Omega$  equals a zero of  $J_0$ , the average velocity vanishes [29]. In this section we investigate how dynamical localization [4,29–32] manifests itself in the free particle absorption spectra. Recently, Meier et al. [33] presented results of a detailed numerical solution of the semiconductor Bloch equations, including excitonic effects, and found that at dynamical localization the relative motion exciton wave function changes from a 3D-character (i.e., localized in  $k_z$ -space) to a 2D-structure (extended in  $k_z$ -space), and below we shall illustrate how the same phenomenon reflects itself in the present analytic study of free-particle properties.

### A. Generalized Density of States

The starting point for our analysis is the effective dispersion (54) introduced in section IV B which we reproduce here for the convenience of the reader,

$$\epsilon_{\text{eff}}[\vec{k}] = \frac{1}{2}\lambda_{\text{eff}} \cos(ak_{\parallel}) + \frac{\hbar^2 k_{\perp}^2}{2m_{\text{eff}}} + \epsilon_g. \quad (84)$$

Henceforth we put  $\epsilon_g = 0$  and drop the “eff” subscript. We consider the effect of the THz field described by the vector potential  $\vec{A}(t) = -\vec{E} \sin(\Omega t)/\Omega$  where  $\vec{E} = (0, 0, E_{\parallel})$ . In accordance with Section IV we calculate the generalized density of states from

$$\rho^{sl}(T, \tau) = \frac{m}{2\pi^2 \hbar^3} \int_0^\infty d\epsilon_{\perp} \int_0^{2\pi/a} dk_{\parallel} e^{-i\epsilon_{\perp}\tau/\hbar} \times \exp[I(T, \tau)], \quad (85)$$

$$I(T, \tau) = -i \frac{\lambda}{2\hbar} \int_{T-\tau/2}^{T+\tau/2} ds \cos[ak_{\parallel} + \gamma \sin(\Omega s)]. \quad (86)$$

We evaluate the integral within the exponential using the identity (64) with the result

$$I(T, \tau) = \frac{\lambda}{2\hbar\Omega} \left\{ \cos(ak_{\parallel}) [\mathcal{C}(\Omega\tau) + J_0(\gamma) \frac{\lambda\tau}{2\hbar}] + \sin(ak_{\parallel}) \mathcal{S}(\Omega\tau) \right\}, \quad (87)$$

where

$$\mathcal{C}(z) = 2 \sum_{n=1}^{\infty} \frac{J_{2n}(\gamma) \cos[2n\Omega T]}{n} \sin[nz] \quad (88)$$

$$\mathcal{S}(z) = 2 \sum_{n=1}^{\infty} \frac{J_{2n-1}(\gamma) \sin[(2n-1)\Omega T]}{n-1/2} \times \sin[(n-1/2)z]. \quad (89)$$

We have suppressed the explicit dependence of  $\Omega T$  and  $\gamma$  in  $\mathcal{C}(z)$  and  $\mathcal{S}(z)$  for simplicity. Note that both of these functions are anti-symmetric in  $z$ , i.e.,  $\mathcal{C}(-z) = -\mathcal{C}(z)$  and  $\mathcal{S}(-z) = -\mathcal{S}(z)$ . The identity [24]

$$\int_0^{2\pi} \frac{d\theta}{2\pi} \exp\{ia \cos\theta + ib \sin\theta\} = J_0(\sqrt{a^2 + b^2}) \quad (90)$$

is the key to the next step in the evaluation of (85) and allows us to write

$$\rho^{sl}(T, \tau) = \frac{m}{2\pi^2 \hbar^3 a} \int_0^\infty d\epsilon_{\perp} e^{-i\epsilon_{\perp}\tau/\hbar} \mathcal{K}(\Omega\tau) \quad (91)$$

where we have defined the kernel

$$\mathcal{K}(z) = J_0 \left( \frac{\lambda}{2\hbar\Omega} \sqrt{(\mathcal{C}(z) + J_0(\gamma)z)^2 + \mathcal{S}^2(z)} \right). \quad (92)$$

Also here we have suppressed the explicit dependence of  $\Omega T$  and  $\gamma$ . In distribution sense we can write

$$\int_0^\infty d\epsilon_{\perp} e^{-i\epsilon_{\perp}\tau/\hbar} = \frac{-i\hbar}{\tau - i0^+}, \quad (93)$$

where  $0^+$  indicates a positive infinitesimal. This expression allows us compute the Fourier transform of (91):

$$\rho^{sl}(T, \epsilon) = \frac{m}{2\pi^2 \hbar^2 a} \left( \int_{-\infty}^{\infty} d\tau \frac{\sin(\epsilon\tau/\hbar)}{\tau} \mathcal{K}(\Omega\tau) + \pi \right). \quad (94)$$

In what follows we shall examine several properties of this result.

## B. The field-free limit

In the limit of vanishing field strength we have

$$\lim_{\gamma \rightarrow 0} \mathcal{K}(z) = J_0 \left( \frac{\lambda z}{2\hbar\Omega} \right). \quad (95)$$

Using the identity [24]

$$\int_{-\infty}^{\infty} \frac{dx}{x} \sin(\beta x) J_0(x) = \begin{cases} \pi & [\beta > 1] \\ 2 \arcsin \beta & [\beta^2 < 1] \\ -\pi & [\beta < -1] \end{cases} \quad (96)$$

we obtain the density of states for a tight-binding superlattice,

$$\rho^{sl}(\epsilon) = \frac{m}{\pi\hbar^2 a} \begin{cases} 1 & [\epsilon > \lambda/2] \\ \frac{1}{\pi} \arcsin(2\epsilon/\lambda) + 1/2 & [|\epsilon| \leq \lambda/2] \\ 0 & [\epsilon < -\lambda/2] \end{cases} \quad (97)$$

which is familiar.

## C. The static limit

In the limit  $\Omega \rightarrow 0$  one obtains

$$\lim_{\Omega \rightarrow 0} \mathcal{K}(\Omega\tau) = J_0 \left( \frac{\lambda}{2\hbar\omega_B} \sin(\omega_B\tau) \right). \quad (98)$$

Recalling the identities [24]

$$J_0(z \sin \alpha) = \sum_j J_j^2(z/2) \cos(2k\alpha) \quad (99)$$

and

$$\int_{-\infty}^{\infty} dx \cos(\alpha x) \sin(\beta x) / x = \pi[\theta(\alpha + \beta) - \theta(\alpha - \beta)], \quad (100)$$

we obtain the density of states

$$\rho^{sl}(\epsilon) = \frac{m}{\pi\hbar^2 a} \sum_j J_j^2 \left( \frac{\lambda}{4\hbar\omega_B} \right) \theta(\epsilon + 2j\hbar\omega_B). \quad (101)$$

This result coincides with the one obtained in Refs. [34,35], which study both theoretically and experimentally the effects of strong static fields on the absorption in superlattice structures. They conclude that the step-like behavior of (101) is due localization in the growth direction (Wannier-Stark localization).

## D. Dynamic localization

As seen in the previous subsection the signature of localization in the growth direction in a superlattice is a step-like behavior of the density of states. This is intuitively clear since the density of states for a 2D system (75) is constant. We therefore expect the density of states to be composed of a step function for each well the states extend into, with weight relative to the occupation in that particular well. We shall now show that if  $J_0(\gamma) = 0$ , i.e., the conditions for dynamical localization are met, then the GDOS indeed is of this kind. The argument runs as follows. If  $J_0(\gamma) = 0$  then the kernel (92) is periodic in  $z$  with period  $2\pi$ . Furthermore, the kernel is an even function:  $\mathcal{K}(z) = \mathcal{K}(-z)$ . We can therefore formally write

$$\mathcal{K}(\Omega\tau) = \sum_j \mathcal{K}_j \cos(k\Omega\tau),$$

which is of the same functional form as in the static limit, Eq.(98). Consequently, we may conclude that the generalized density of states must be of the form

$$\rho_{dyn.loc}^{sl}(\epsilon) = \frac{m}{\pi\hbar^2 a} \sum_j \mathcal{K}_j \theta(\epsilon + j\hbar\Omega), \quad (102)$$

i.e., it is a superposition of step-functions. The weights  $K_j$ , however, must be evaluated numerically, and examples are given in the next section. It is important to note that the “step-length” in the ac-case is determined by the frequency of the THz-field in contrast to the static case, where it is determined by the field strength. The field strength enters the density of states only through the weight-factors  $K_j$ .

The result (102) suggests that it should be possible to probe dynamic localization by photo-absorption: when the appropriate conditions are approached, the absorption coefficient should change qualitatively from a generic smooth behavior to a sharply defined step-like structure. The number of distinct steps appearing in the spectrum is determined by the ratio  $\lambda/\hbar\Omega$  which is also a measure of the number of wells the localized states span. This is fully consistent with the results of [33], who considered a miniband of width  $\lambda = 21\text{meV}$  and FIR frequency  $\hbar\Omega = 20\text{meV}$ , which corresponds to a single step, and hence maximum binding energy of the corresponding exciton which would be mostly confined to a single well.

## E. Numerical results

We again focus our numerical study to the time averaged generalized density of states  $\rho_{ave}^{sl}(\epsilon) = \frac{\Omega}{2\pi} \int_0^{2\pi/\Omega} dT \rho^{sl}(T, \epsilon)$ . In Figs. 6 and 7 we show the absorption spectra for a superlattice with effective bandwidth  $\lambda = 3.4\hbar\Omega$ . The numerical results confirm the expectations of the previous section: when the  $\gamma =$

$aeE_{||}/\hbar\Omega$  approaches the first zero of  $J_0$ , which occurs at the argument value of 2.4048.., the gradually evolving replicas of the zero-field density of states converge into plateaus of finite width. The exactness of the plateaus can be judged from Fig. 7: at  $\gamma = 2.4048..$  the line joining the the steps appears near vertical. Finally, in Fig. 8 we show the DTS spectra at dynamical localization (DL) and non-DL conditions. There are two characteristic differences: (i) Outside the zero-field miniband DL leads to a step-like structure in contrast to the smooth behavior found otherwise, and (ii) Inside the miniband the DL-spectrum distinguishes itself by its sharp jagged structure.

## VII. CONCLUSIONS

We have presented a theoretical formulation of linear photo-absorption for samples under strongly non-equilibrium conditions. Typical non-equilibrium agents would be THz-radiation from free-electron lasers, or ultra-short pulse measurements of transient effects. In the present work noninteracting carriers are considered, but the formulation allows an extension to Coulomb interactions, which will be addressed in our future work. Two central concepts emerge from our analysis: a generalization of the density of states into time-dependent conditions [GDOS defined in Eq.(56)], and photonic side-bands, which form a convenient framework for discussing the various features of the absorption spectra.

## ACKNOWLEDGMENTS

We wish to acknowledge useful discussions with Ben Hu, Andreas Wacker and Björn Birnir. Furthermore we wish to thank Fausto Rossi and Junichiro Kono for valuable comments of an earlier version of the manuscript and Kent Nordstrom for sharing details of his unpublished data [16]. This work was partially supported by a LACOR grant no. 4157U0015-3A from Los Alamos National Laboratory.

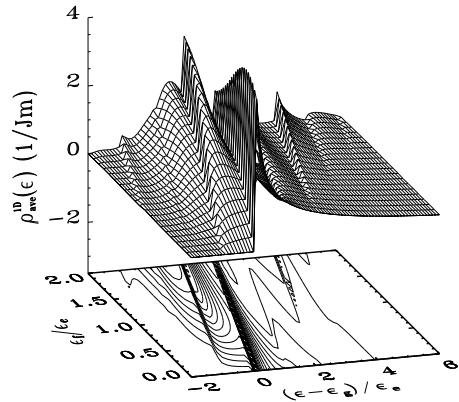


FIG. 1. Time averaged generalized density of states for 1D-system shown for a range of FIR-intensities,  $\epsilon_f/\hbar\Omega \in [0, 2]$ . The band edge and the side-bands display a blue-shift, which scales linearly with the intensity. Absorption extends below the bandgap (dynamical Franz-Keldysh effect).

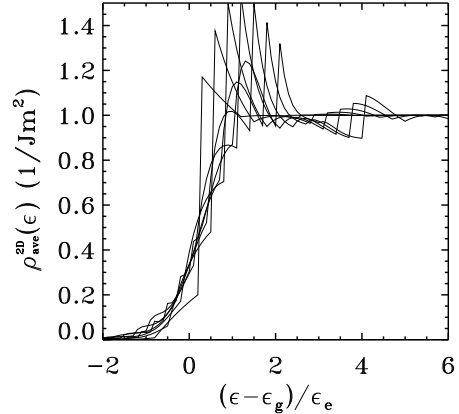


FIG. 2. The time averaged GDOS for a 2D-system for a range of FIR-intensities,  $\epsilon_f/\hbar\Omega = (0.2, 0.5, 0.8, 1.1, 1.4, 1.7, 2.0)$ . At low intensities one observes a Stark-like blue-shift of the band edge as well as finite absorption within the band gap. With increasing intensity side bands emerge at  $\epsilon = \epsilon_g + \epsilon_f \pm 2\hbar\Omega$ .

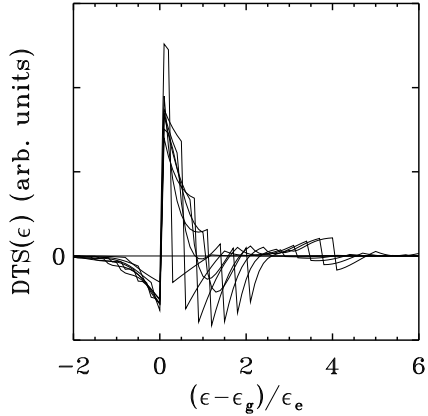


FIG. 3. The DTS signal for a 2D-system for a range of intensities,  $\epsilon_f/\hbar\Omega = (0.2, 0.5, 0.8, 1.1, 1.4, 1.7, 2.0)$ .

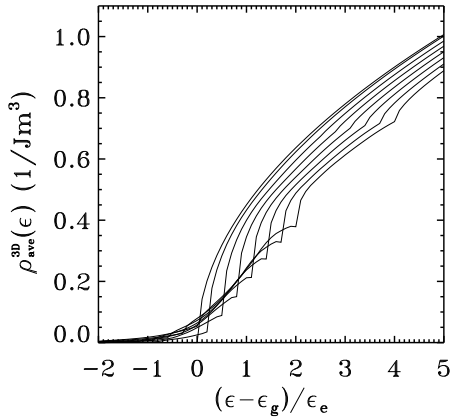


FIG. 4. The time averaged generalized density of states for a 3D-system for a range of FIR-intensities,  $\epsilon_f/\hbar\Omega = (0.0, 0.2, 0.5, 0.8, 1.1, 1.4, 1.7, 2.0)$ .

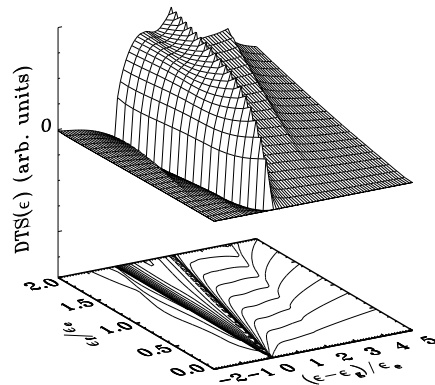


FIG. 5. DTS-spectrum for a 3D-system.

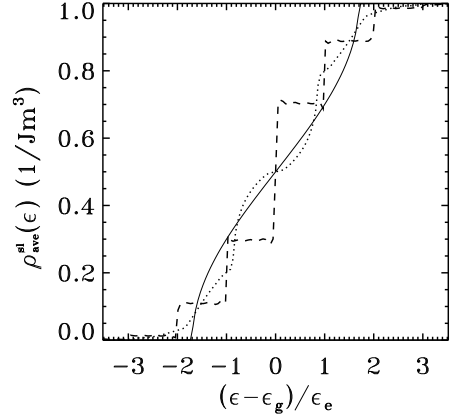


FIG. 6. The time-averaged GDOS for a superlattice with effective band-width  $\lambda = 3.4\hbar\Omega$ . Dots:  $\gamma = 1.5$ ; dashes:  $\gamma = 2.4$ . The proximity of dynamical localization occurring at  $\gamma = 2.4048\dots$  reflects itself in the step-wise structure of the dashed curve.

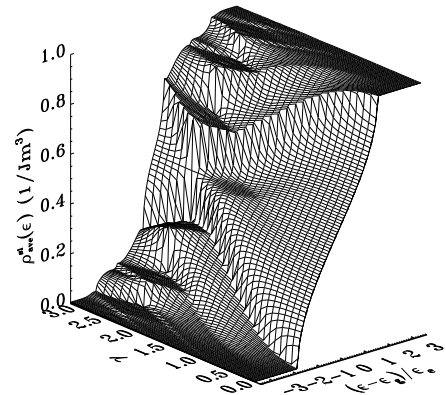


FIG. 7. The time averaged GDOS for a superlattice with  $\lambda = 3.4\hbar\Omega$  as a function of FIR-intensity. At low  $\gamma$  side bands are observed, which merge at  $\gamma = 2.4048\dots$  corresponding to dynamical localization.

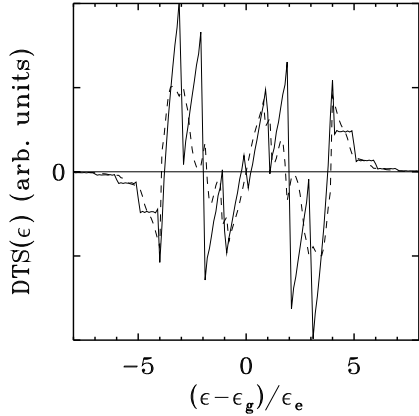


FIG. 8. The differential transmission signal for superlattice structure with effective mini bandwidth  $\lambda = 8\hbar\Omega$ . Solid line:  $\gamma = 2.4$ ; dashes:  $\gamma = 2.0$ . Outside the zero-field mini-band a step-like behavior is seen, while inside the mini-band DTS for dynamical localization develops a jagged shape in contrast to the smooth behavior for the extended state.

Confusion can be avoided by noting that in the case of complex-time variables the Green functions have a superscript  $c$ , while in the real-time case they have  $r, a$ , or  $<$ .

- [18] H. Haug and S. W. Koch, *Quantum theory of the optical and electronic properties of semiconductors* (World Scientific, Singapore, 1993).
- [19] T. Kuhn and F. Rossi, Physical Review Letters **69**, 977 (1992); *ibid.* **72**, 152 (1994); S. Haas *et al.*, Phys. Rev. B **53**, 12855 (1996).
- [20] See, e.g., Chapter 11 in Ref. [12].
- [21] S. Schmitt-Rink, D. S. Chemla, and D. A. Miller, Adv. Phys. **38**, 89 (1989).
- [22] J. H. Davies and J. W. Wilkins, Phys. Rev. B **38**, 1667 (1988).
- [23] R. Bertoncini and A.-P. Jauho, Phys. Rev. B **44**, 3655 (1991).
- [24] I. S. Gradshteyn and I. M. Ryzhik, *Table of Integrals, Series and Products* (Academic Press, New York, 1994), 5th ed.
- [25] M. Wagner, Phys. Rev. Lett. **76**, 4010 (1996); J. Iñarrea and G. Platero, Europhys. Lett. **34**, 43 (1996).
- [26] It is interesting to note that by comparing the GDOS in the 2D and 3D case with Eqs. (15-18) in [6] one may obtain exact expansions for the integrals in terms of Bessel functions.
- [27] K. Unterrainer *et al.*, Phys. Rev. Lett. **76**, 2973 (1996).
- [28] C. Waschke *et al.*, Phys. Rev. Lett. **70**, 3318 (1993).
- [29] A. A. Ignatov and Y. A. Romanov, Phys. Status Solidi (b) **73**, 327 (1976); D. H. Dunlap and V. M. Kenkre, Phys. Rev. B **34**, 3625 (1986).
- [30] X.-G. Zhao, J. Phys.: Condens. Matter **6**, 2751 (1994).
- [31] M. Holthaus, G. W. Ristow, and D. W. Hone, Europhys. Lett. **32**, 241 (1995).
- [32] J. Rotvig, A.-P. Jauho, and H. Smith, Phys. Rev. Lett. **74**, 1831 (1995); Phys. Rev. B **54**, 17691 (1996).
- [33] T. Meier, F. Rossi, P. Thomas and S. W. Koch, Phys. Rev. Lett. **75**, 2558 (1995).
- [34] J. Bleuse, G. Bastard, and P. Voisin, Phys. Rev. Lett. **60**, 220 (1988).
- [35] P. Voisin *et al.*, Phys. Rev. Lett. **61**, 1639 (1988).

[1] J. Cerne *et al.*, Phys. Rev. B **51**, 5253 (1995).  
[2] P. S. S. Guimarães *et al.*, Phys. Rev. Lett. **70**, 3792 (1993); B. J. Keay *et al.*, Phys. Rev. Lett. **75**, 4098 (1995).  
[3] B. J. Keay *et al.*, Phys. Rev. Lett. **75**, 4102 (1995).  
[4] M. Holthaus and D.W. Hone, Phys. Rev. B **49**, 16605 (1994).  
[5] Y. Yacoby, Phys. Rev. **169**, 610 (1968).  
[6] A.-P. Jauho and K. Johnsen, Phys. Rev. Lett. **76**, 4576 (1996).  
[7] J. Kono *et al.*, (unpublished); J. Kono *et al.*, in *Proc. of 23<sup>rd</sup> Int. Conf. on the Physics of Semiconductors*, eds. M. Scheffler and R. Zimmerman (World Scientific, Singapore, 1996), p. 1911.  
[8] B. Birnir *et al.*, Phys. Rev. B **47**, 6795 (1995).  
[9] H. Heesel *et al.*, Phys. Rev. B **47**, 16000 (1993).  
[10] F. X. Camecasse *et al.*, Phys. Rev. Lett. **77**, 5429 (1996).  
[11] For a recent theoretical paper modeling the experiments of Ref. [3] see, e.g., A. Wacker *et al.*, archived in cond-mat/9612035, where also other relevant work is cited.  
[12] H. Haug and A.-P. Jauho, *Quantum Kinetics in Transport and Optics of Semiconductors* (Springer, Berlin, 1996).  
[13] W. Pötz, Phys. Rev. B **54**, 5647 (1996).  
[14] These rules are summarized, e.g., in Table 4.1. of Ref [12].  
[15] H. Haug and S. Schmitt-Rink, Prog. Quantum Electronics **9**, 3 (1984).  
[16] K. Nordstrom *et al.*, (unpublished).  
[17] The reader should note that the symbol  $\tau$  is used in a dual meaning: it can indicate a complex-time variable on the Keldysh contour, or the time-difference variable.